

Toward Development of Targeted Nonsteroidal Antiandrogen-1,4,7,10-Tetraazacyclododecane-1,4,7,10-tetraacetic Acid–Gadolinium Complex for Prostate Cancer Diagnostics

Hanit Marom,[†] Keren Miller,[‡] Yossi Bechor-Bar,[†] Galia Tsarfaty,[§] Ronit Satchi-Fainaro,^{*,‡} and Michael Gozin^{*,†}

[†]*School of Chemistry, Raymond and Beverly Sackler Faculty of Exact Sciences, Tel Aviv University, Tel Aviv 69978, Israel,*

[‡]*Department of Physiology and Pharmacology, Sackler School of Medicine, Tel Aviv University, Tel Aviv 69978, Israel, and*

[§]*Imaging Radiology, Chaim Sheba Medical Center, Ramat Gan, Israel*

Received July 6, 2009

Androgen receptors are present in most advanced prostate cancer specimens, having a critical role in development of this type of cancer. For correct prognosis of patient conditions and treatment monitoring, noninvasive imaging techniques have great advantages over surgical procedures. We developed synthetic methodologies for preparation of novel androgen receptor-targeting agents in an attempt to build a versatile platform for prostate cancer imaging and treatment. The structure of these compounds comprises of a lanthanoid metal ion, gadolinium-1,4,7,10-tetraazacyclododecane-1,4,7,10-tetraacetic acid (Gd-DOTA)-based binding fragment and, connected to it by a flexible linker, bicalutamide-derived nonsteroidal antiandrogen moiety. A representative gadolinium complex **15** was evaluated as a magnetic resonance imaging (MRI) agent in C57/bl6 male mouse bearing orthotopic TRAMP C2 prostate tumor.

Introduction

Prostate cancer continues to have the highest incidence rate of any other type of cancer in males, and it is the second leading cause of cancer deaths in male (in the United States), with approximately 220000 new cases diagnosed each year only in US.¹ The normal development and maintenance of the prostate is dependent on androgen acting through the androgen receptor (AR^a), which remains important in the development and progression of prostate cancer. AR expression is maintained throughout prostate cancer progression, and the majority of androgen-independent or hormone refractory prostate cancers express AR.² New imaging modalities for the prostate cancer are needed in order to avoid unnecessary treatment, correctly stage and predict disease course, and develop more effective therapies.

Several important criteria should be considered when potential biomarkers are chosen for development as clinical tools. In this respect, one of the most important issues is the quality of scientific and clinical data supporting selected biomarker potential utility. Another important criterion is that a biomarker presence could be conveniently detected by widely available assays or techniques, providing useful and readily accessible and interpretable information to clinicians.^{3–7}

AR ligands can be divided into two main structural classes, steroidal and nonsteroidal, and into two different functional classes, androgenic and antiandrogenic.^{8,9} Principal therapeutic approaches that are common for a progressive prostate cancer treatment and results in the regression of most androgen-dependent tumors¹⁰ include an androgen ablation monotherapy (using a single drug for a treatment) and surgical or chemical castration with nonsteroidal antiandrogens, such as flutamide and bicalutamide. Nonsteroidal antiandrogens such as flutamide, nilutamide, and bicalutamide were shown to bind exclusively to the AR and therefore having few side effects.

Presently, bicalutamide is the leading antiandrogen used in clinical practice, and although it is given as a racemic mixture, the *R*-enantiomer of the bicalutamide was found to have 30-fold higher binding affinity (11 ± 1.5 nM) to the androgen receptor than its *S*-stereoisomer.^{11–17}

Antibodies directed to prostate-specific targets have applications as imaging and therapeutic agents. The advantages of antibody-based imaging techniques include great versatility in target selection. Also, in the case of monoclonal antibodies, each molecule has the same specificity and binding affinity to its target antigen. Main disadvantages of antibody-based approach relate to a relatively high complexity of production and cost of these materials, which frequently hinder a commercial development. Furthermore, antibodies may suffer from inherently problematic pharmacokinetics, which manifested in a limited access to tumors and slow washout rates, resulting in a significant background radioactivity.

Efforts to develop effective radiopharmaceuticals for prostate cancer diagnostics led to approval of ¹¹¹indium-labeled prostate-specific membrane antigen (PSMA) monoclonal antibody (ProstaScint) as an imaging agent.^{18–21} The overall sensitivity and specificity of this tracer has been widely variable in reported studies and, as a result, ProstaScint is not

*To whom correspondence should be addressed. For M.G.: phone, +972-3-640-5878; fax, +972-3-640-5879; E-mail, cogozin@mgchem.tau.ac.il.

^aAbbreviations: DOTA, 1,4,7,10-Tetraazacyclododecane-1,4,7,10-tetraacetic acid; MRI, magnetic resonance imaging; AR, androgen receptor; PSMA, prostate-specific membrane antigen; PET, positron emission tomography; SPECT, single photon emission computerized tomography; HBTU, *O*-benzotriazole-*N,N,N,N*-tetramethyl-uronium-hexafluorophosphate; HOBt, *N*-hydroxybenzotriazole; DCC, dicyclohexylcarbodiimide; MALDI-TOF, matrix assisted laser desorption/ionization time-of-flight; HPLC, high pressure liquid chromatography.

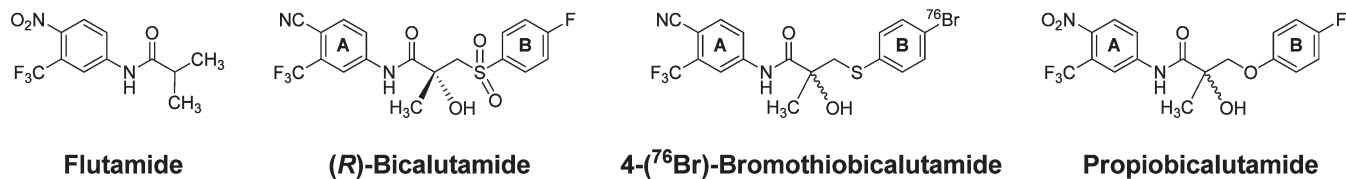


Figure 1. Structures of nonsteroidal antiandrogens. Flutamide, (*R*)-bicalutamide, racemic 4-[⁷⁶Br]-bromothiobicalutamide, and racemic propiobicalutamide.

routinely used for prostate cancer staging.⁹⁰ Yttrium-labeled PSMA monoclonal antibody J591 was also evaluated in clinical trials.²² In a latter case, although bone metastases were imaged in 7 out of 12 patients, only a minority of total individual lesions were detected.

An alternative approach to radiolabeled antibodies is focused on development of androgen receptor radioligands for positron emission tomography (PET) and single photon emission computerized tomography (SPECT)-based imaging of the prostate. This includes evaluation of steroidal compounds such as 16 β -[¹⁸F]fluoro-5 α -dihydrotestosterone^{23,24} and nonsteroidal agents, based on flutamide and bicalutamide pharmacophores such as (*R*)-[¹⁸F]-hydroxyflutamide, (*R*)-[¹¹C]-dimethylamino-hydroxy-flutamide derivatives, (\pm)-3-[⁷⁶Br]-bromohydroxyflutamide, [¹⁸F]-bicalutamide, [⁷⁶Br]-bromo-bicalutamide, and [⁷⁶Br]-bromothiobicalutamide.^{25–29} The [⁷⁶Br]-bromobicalutamide compound was found to have an order of magnitude higher affinity for AR, as compared to that of bicalutamide (K_d of 0.113 μ M for [⁷⁶Br]-bromobicalutamide versus to K_d of 1.276 μ M for bicalutamide). Also, very recently, a series of novel prospective SPECT imaging agents was reported. These ^{99m}Tc-containing flutamide derivatives were synthesized, characterized, and evaluated, showing a significant selective uptake by a prostate. Yet, to the best of our knowledge, no reports regarding development of AR-targeted contrast agents for MRI are available.

Here we report development of nonsteroidal antiandrogen–lanthanoid metal complexes as potential imaging contrast agents for prostate cancer diagnostics. The nonsteroidal antiandrogen-derived targeting moiety was selected as a platform because androgenic steroids tend to bind also to other steroid receptors.³⁰ Additional advantage of our approach is that the same ligand could be suitable for both imaging and treatment procedures depending on the used metal ion.^{31–34}

Results and Discussion

The selection and design of our receptor-targeting moiety was based on work of Miller and co-workers, who synthesized and tested a series of new bicalutamide analogues that have an O-linkage to a B-ring, instead of SO₂-linkage (Figure 1).^{35–39} Replacement of the sulfone with an ether functional group results in compounds that have higher affinity to the androgen receptor, even in comparison with the bicalutamide. The explanation for this activity is that their ether compound forms an intramolecular hydrogen bond with the amide nitrogen which bends the conformation and increase the binding affinity to the receptor. The amide nitrogen and hydroxyl group of (*R*)-bicalutamide have an important hydrogen bonding similar to the trifluoromethyl group on the metaposition of the A ring, which are critical for the interactions between the receptor and ligand.⁴⁰

Considering the binding of the ligand to the receptor we connect a flexible 2,2'-(ethane-1,2-diyl-bis(oxy))diethanamine linker between the targeting and imaging moieties to prevent

possible steric interference of a bulky 1,4,7,10-tetraazacyclododecane-1,4,7,10-tetraacetic acid (DOTA) complex in binding to the receptor (Scheme 1).

As a lanthanoid metal ion-binding moiety, a macrocyclic DOTA ligand was chosen. Metal complexes of this ligand are known to have an exceptional stability, and many of them are clinically used in MRI and PET diagnostics.^{41–45} Other metal-DOTA-based radiopharmaceuticals, such as yttrium ⁹⁰Y-DOTA-tyr3-octreotide, are studied for treatment of various forms of cancer.^{46–48}

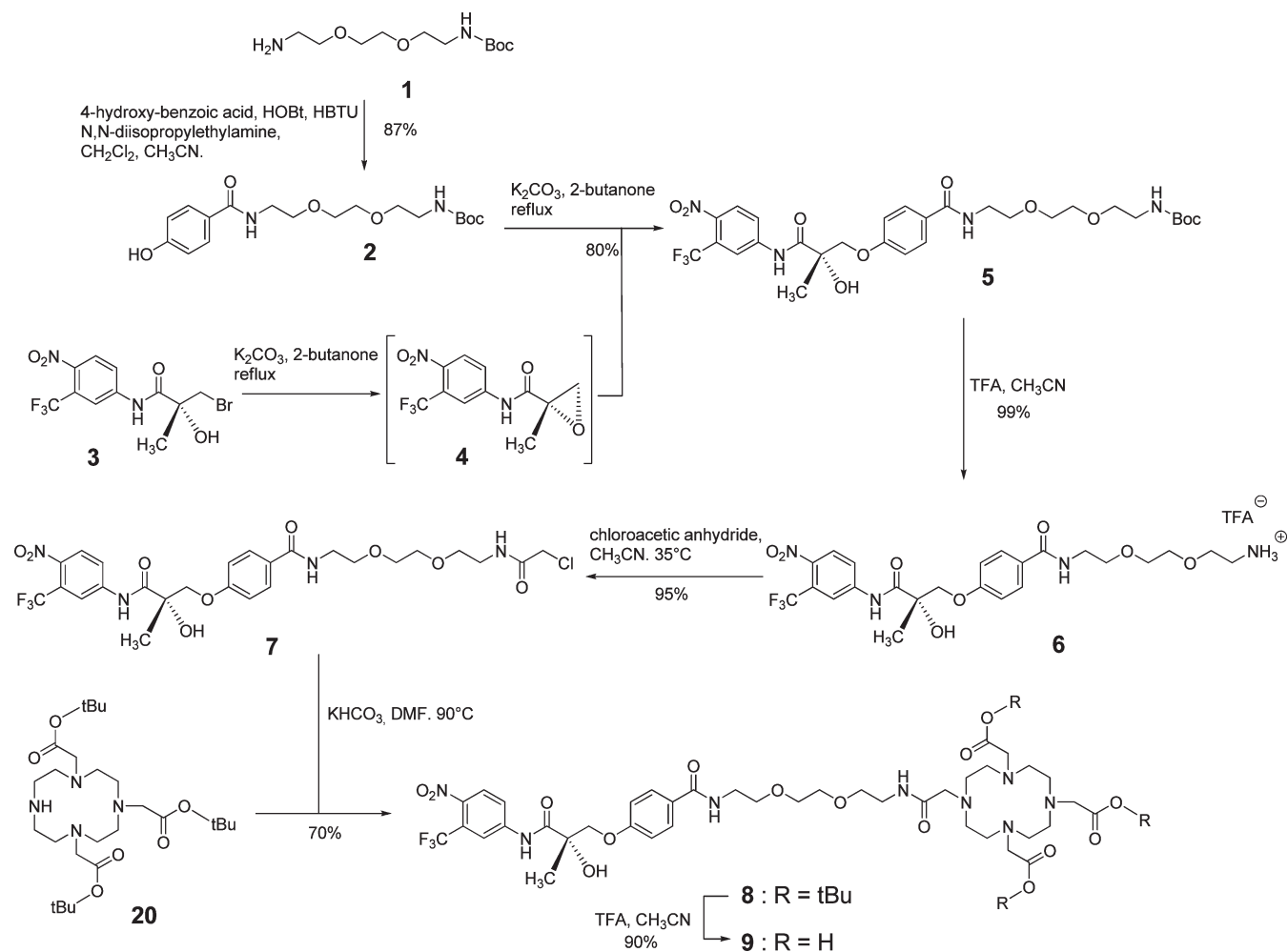
We evaluated two converging synthetic routes (*A* and *B*) for the preparation of the key ligand **9**. *Route A* included six steps and was oriented toward initial derivatization of starting (*R*)-3-bromo-2-hydroxy-2-methyl-*N*-(4-nitro-3-(trifluoromethyl)phenyl)propanamide **3**⁴⁹ into the advanced intermediate **7**, which at later stages of the synthesis was coupled with the commercially available DOTA precursor 1,4,7-tris(*tert*-butoxycarbonylmethyl)-1,4,7,10-tetraazacyclododecane (**20**)⁴⁵ and deprotected to obtain the target ligand **9** (Scheme 1).

This route was initiated with preparation of compound **2**⁵⁰ by coupling of 4-hydroxybenzoic acid with *tert*-butyl-2-(2-(2-aminoethoxy)ethoxy)ethylcarbamate **1**⁵¹ under DCC/HOBt coupling conditions. We found that 4-hydroxybenzoic acid is poorly soluble in CH₂Cl₂ and, as a result, the reaction progress was extremely slow. To improve solubility of this starting material CH₃CN was added as a cosolvent. However, under these new conditions, the formed dicyclohexyl urea side product was soluble, causing serious complications during column chromatography purification of the compound **2**.

Therefore, we turned to an alternative coupling strategy using *O*-benzotriazole-*N,N,N,N'*-tetra-methyluroniumhexafluorophosphate/*N*-hydroxybenzotriazole (HBTU/HOBt) as a coupling reagent and CH₂Cl₂/CH₃CN mixture as a solvent.⁵² The latter protocol was found to have significant advantages over dicyclohexylcarbodiimide (DCC)/HOBt procedure in terms of yield, reaction time, and simplicity of the product purification. Under HBTU/HOBt coupling conditions, the reaction was completed in just 2 h (versus 24 h, using the DCC/HOBt protocol), and after chromatography, pure phenol derivative **2** was obtained in 87% yield.

The second step in development of synthetic *route A* began with attempts to couple compounds **3** and **2** in THF, using *t*-BuOK as a base. Under these reaction conditions, no desired derivative **5** was observed. Instead, we found that all starting aromatic amide **3** underwent complete hydrolysis, producing 4-nitro-3-(trifluoromethyl)benzenamine as the major detectable product.

An alternative strategy for preparation of the derivative **5** was based on in situ preparation of epoxide **4**²⁵ as a precursor. According to Miller's reports¹⁷ and to our own findings, conversion of compound **3** to the corresponding epoxide **4** can be achieved in very high yields by refluxing of **3** with anhydrous K₂CO₃ in a dry acetone. Under these solid–liquid reaction conditions, hydrolysis of the sensitive aromatic amide group

Scheme 1. Route A for the Preparation of Ligand **9**

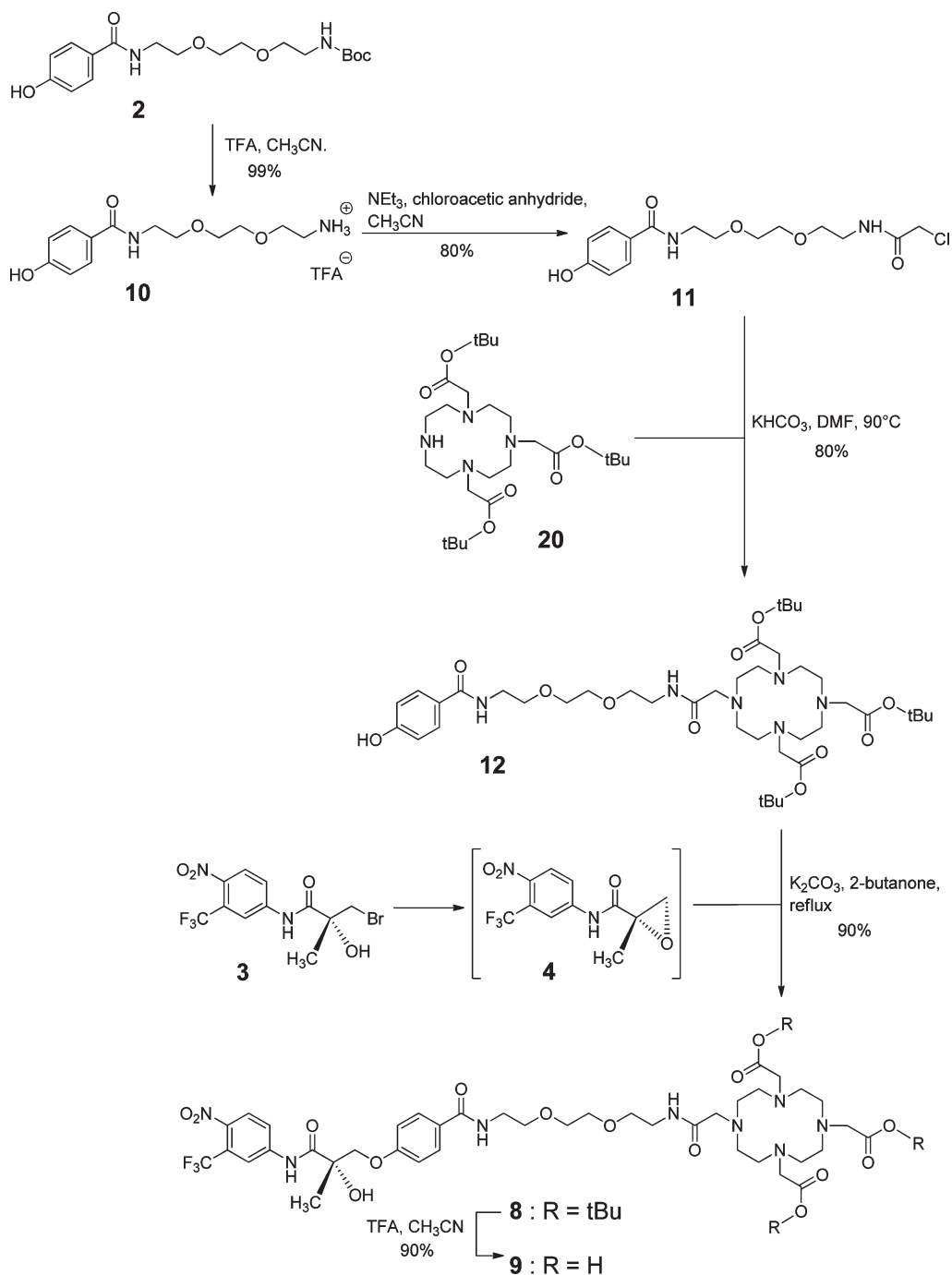
could be mostly avoided. Thus, a solution of compounds **2** and **3** in dry 2-butanone was refluxed overnight in presence of anhydrous K_2CO_3 powder, yielding derivative **5** in 80% isolated yield and clearly indicating a viability of this synthetic approach. It is important to mention that strict anhydrous conditions are critical to the success of the latter reaction, as the presence of water traces drastically reduces the observed yields.

In the next step, the Boc protection group of compound **5** was removed by treatment with trifluoroacetic acid in CH_2Cl_2 , producing compound **6** in a quantitative yield. The subsequent reaction of compound **6** with chloroacetic anhydride in a dry CH_3CN at 35°C (at room temperature this reaction rate was relatively slow) led to formation of chloroacetamide **7** in 95% isolated yield.⁵³ Interestingly, compound **7** was stable under ambient conditions and could be conveniently purified by a silica gel chromatography using CH_3CN as an eluent. ^1H NMR spectra of compound **6** and **7** were practically identical, except for a singlet peak at 4.05 ppm (in $\text{DMSO}-d_6$), which was assigned to a terminal methylenechloride group of compound **7**. As mentioned above, the synthesis toward the target ligand **9** was preceded with heating a solution of **7** and **20** in DMF to 90°C with addition of anhydrous KHCO_3 , as a base.⁵⁴ These optimized conditions for the latter reaction allowed compound **8** to be obtained in 70% yield, while the main detected byproduct was 4-nitro-3-(trifluoromethyl)benzenamine. The hydrolysis of the key

precursor **8** was performed with trifluoroacetic acid in dry CH_3CN at 0°C , leading to overall yield of 42% using *route A* toward ligand **9**.

Our second “inverted” approach: *route B* contained five synthetic steps using compound **2** as a starting material and was oriented toward derivatization of the DOTA precursor **20** into the advanced intermediate **12**, which at later stages of the synthesis, was coupled with compound **3** and deprotected to obtain the target ligand **9** (Scheme 2).

The second strategy (*Route B*) for synthesis of the compound **9** was initiated with deprotection of Boc group of the compound **2** using trifluoroacetic acid in CH_3CN and producing intermediate **10** in a quantitative yield. Subsequently, treatment of the latter material with chloroacetic anhydride in CH_3CN led to formation of chloroacetamide **11** in 80% isolated yield. Compound **11** in DMF was then heated to 90°C in the presence of **20** and K_2CO_3 , affording derivative **12** in 80% yield. Then, reaction of an in situ-generated chiral epoxide **4** with compound **12** in 2-butanone led to formation of the key precursor **8**. Conversion of compound **8** to the target ligand **9**, described in the above protocol, resulted in overall yield of 51% using *route B*. An additional and seemingly more straightforward synthetic route that we evaluated was based on coupling of compound **6** with another commercially available precursor, 1-(ethyl acetic)-4,7,10-tris-(*tert*-butoxycarbonylmethyl)-1,4,7,10-tetraazacyclododecane (**21**). According to our above-mentioned experience, we

Scheme 2. Synthetic Route B for the Preparation of the Ligand 9

attempted to use HOBt and HBTU coupling reagents (Scheme 3).

Unexpectedly, chromatographic monitoring of this reaction revealed formation of significant amount of various byproducts, resulting in low yields of the desired product **8**, even after prolonged reaction times. Many attempts were made to improve this reaction outcome by trying a series of solvents and coupling reagents. However, in all these experiments, only complex mixtures of products were observed. Moreover, while reversed-phase flash chromatography could not provide sufficient separation, under any evaluated elution conditions, some of the obtained byproducts were found to be unstable on a normal phase silica gel support, undergoing decomposition and complicating even further the purification

process. We concluded that previously described routes A and B were superior methodologies for the preparation of the target ligand **9**.

Our additional task was to prepare a DOTA–lanthanoids metal complex that has structural similarity to target complex but would lack the receptor-targeting moiety. This complex is an optimized control for biological experiments (Scheme 4, left).

Synthesis of gadolinium complex **14** was achieved by heating an aqueous solution of ligand **13** (buffered to pH 5) with gadolinium acetate salt.⁵⁵ After water lyophilization and reversed phase chromatography, complexes **14** was obtained in excellent yields (above 90%). For the preparation of the target complex **15**, the same protocol was used, giving a typical

yield in a range of 50%. Identity of the gadolinium complexes was established by matrix assisted laser desorption/ionization time-of-flight (MALDI-TOF) mass spectrometry.

To evaluate the binding capability of complex **15** to the AR, we performed a series of in vitro quantitative immunoprecipitation AR-binding experiments, in which complex **15** and bicalutamide nitro analogue (*R*)-3-((4-fluorophenyl)sulfonyl)-2-hydroxy-2-methyl-*N*-(4-nitro-3-(trifluoro-methyl)-phenyl)-propanamide (**22**)¹² were separately incubated with resin-bound AR, as described by Reddy and co-workers.⁵⁶ Following this noncompetitive binding protocol (flowcharts of which are shown in Figure S75 of the Supporting Information), AR complexes of compounds **15** or **22** were selectively precipitated by AR's monoclonal antibody, bound to protein G-Sepharose resin (compound **14** was tested as a reference in control immunoprecipitation experiments). The amounts of unbound antiandrogens, which remained in the solution, were quantitated by high pressure liquid chromatography (HPLC). To correct results of our assay for a non-specific binding of the evaluated antiandrogens to other proteins or assay's components, the same set of experiments was

performed without addition of the AR. The difference between integration areas under the curve (AUC) in AR-added

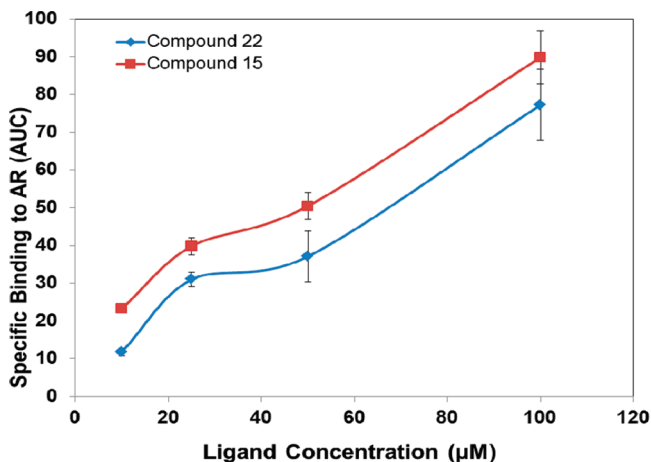
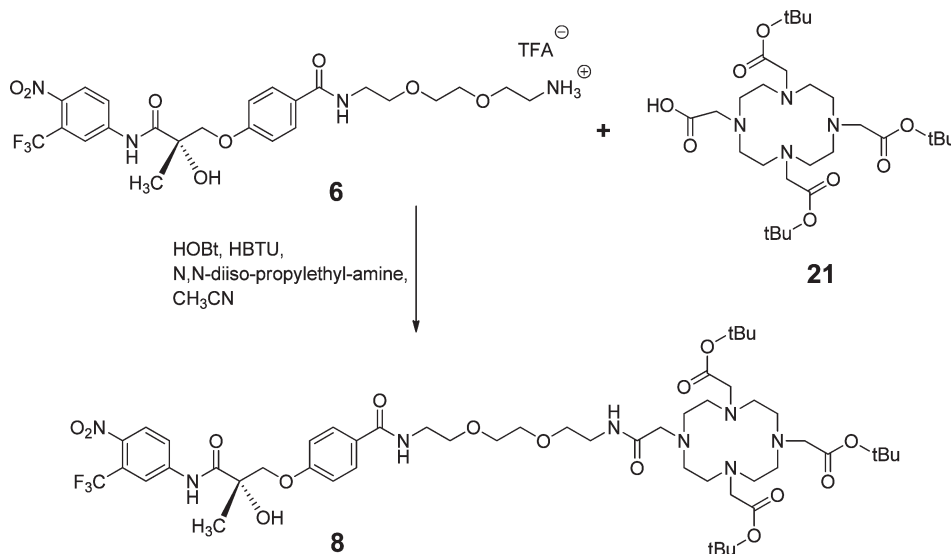
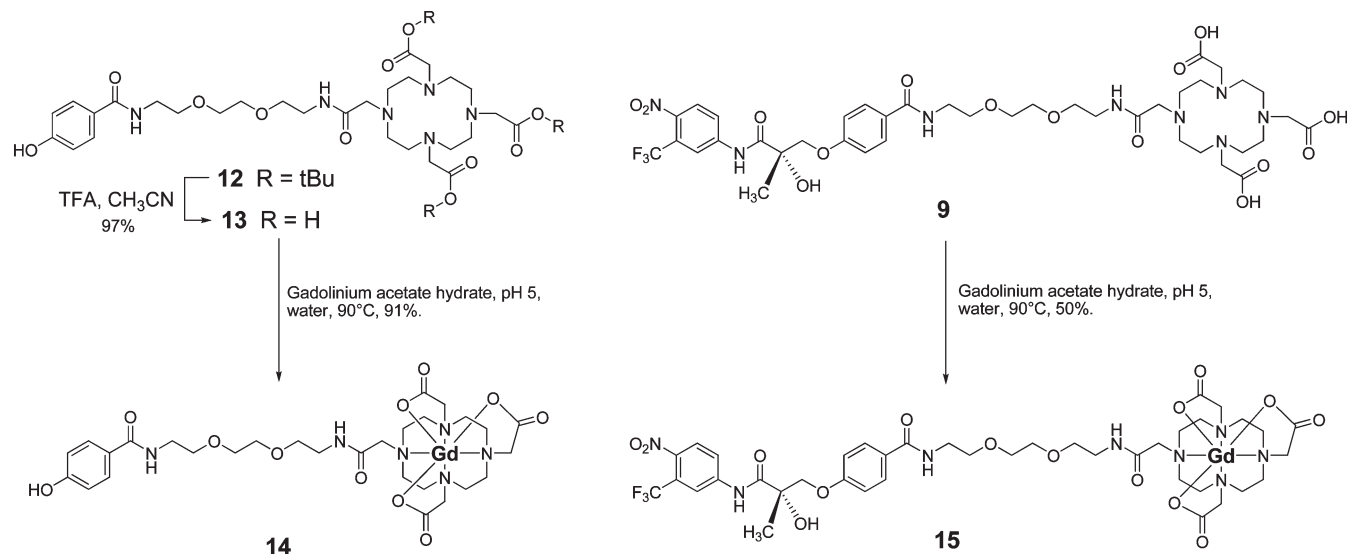


Figure 2. Results of the immunoprecipitation AR binding experiments with compounds **15** and **22**.

Scheme 3. Alternative Synthesis of Compound **8**



Scheme 4. Synthesis of Ligand **13** and Corresponding Complex **14** (left); Synthesis of Corresponding Complex **15** (right)



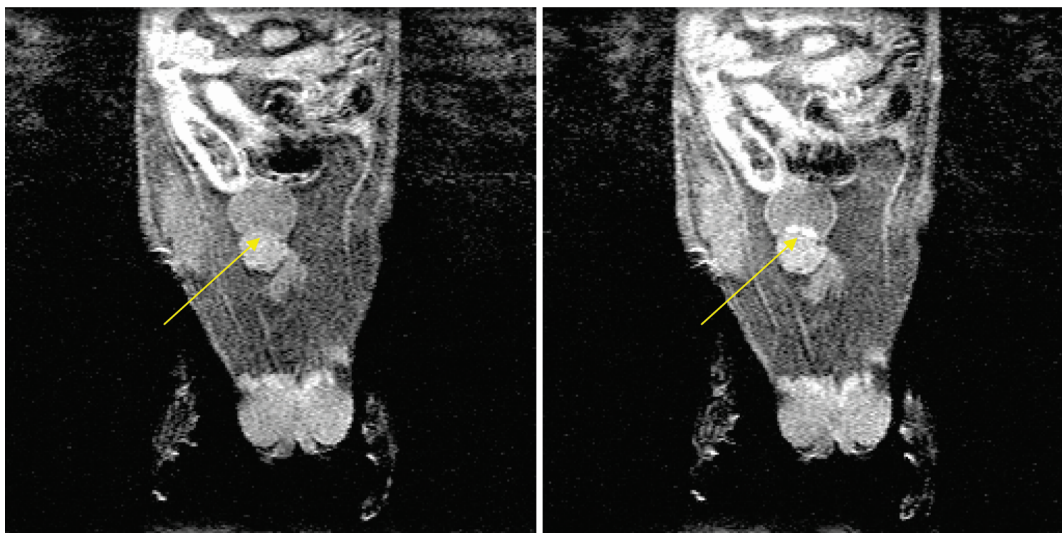


Figure 3. Accumulation of the complex **15** in mouse prostate tumor. MRI of mouse prostate tumor prior to complex **15** injection (left); MRI of mouse prostate tumor 7 min after complex **15** injection (right).

and AR-free yields the specific AR-binding affinity for each evaluated antiandrogen at each concentration (Figure 2 and Tables S1–S3 of the Supporting Information).

We found that in a range of concentrations of 10–100 μM , compounds **15** and **22** exhibited similar affinity to the AR. However, above 250 μM concentration, both **15** and **22** showed a nonlinear binding-concentration response, possibly due to partial precipitation of these ligands at such concentrations, under our experimental conditions. All binding experiments were performed in triplicates, and averaged values are presented as the mean \pm standard deviation. Overall, data of our binding studies strongly suggested that compound **15** may act as in vivo contrast agent in a prostate cancer imaging.

To test whether complex **15** targets prostate tumors, preliminary in vivo imaging experiment was performed. TRAMP C2 cells¹⁹ (1.5×10^6 cells) were implanted into the prostate of C57/bl6 male mouse.⁵⁷ Four weeks post implantation, the C57/bl6 mouse (25 g) bearing orthotopic TRAMP C2 prostate tumor was injected with 6.25 mM solution (500 μL ; 0.125 mmol/kg⁵⁸) of gadolinium complex **15** and imaged every few minutes.

As can be seen in Figure 3 (right), a slight enhancement of the prostate tumor region was observed at this concentration of complex **15**.

Conclusions

Our investigations present unprecedented synthesis of prostate-targeted nonsteroidal antiandrogen-DOTA–gadolinium complex **15** designed for prostate cancer magnetic resonance imaging. Binding studies comparing affinity of complex **15** and reference compound **22** clearly showed that both these materials have similar affinity toward AR. Finally, our preliminary in vivo evaluation of gadolinium complex **15** as a prostate imaging contrast agent has been conducted in C57/bl6 mouse, bearing orthotopic TRAMP C2 prostate tumor. We believe that use of prostate-targeting ligand **9** complexes, containing appropriate radioactive metal ions, could be also very promising for PET- and SPECT-based imaging of prostate tumors. Our study paves the way for the introduction of novel “dual-purpose” receptor-targeted pharmaceutical precursors (metal chelators), which depending on a dosage and utilized metal ions, are designed to be suitable for

diagnostics or therapy. To further evaluate this type of compounds performance as potential therapeutic agents, additional experiments are planned to study these materials stability, target-specificity, and metabolism.

Experimental Section

All operations with air- and moisture-sensitive compounds were performed by the Schlenk techniques under argon atmosphere. All solvents were of analytical grade or better. Toluene and THF were distilled over sodium/benzophenone; other solvents were purchased as anhydrous. ^1H and ^{13}C NMR spectra were recorded on 200, 400, or 500 MHz spectrometers in CDCl_3 , CD_3OD , or $\text{DMSO}-d_6$. ^1H and ^{13}C NMR signals are reported in ppm. ^1H NMR signals are referenced to the residual proton (7.26 ppm for CDCl_3 or 2.50 ppm for $\text{DMSO}-d_6$ or 3.31 ppm for CD_3OD) of a deuterated solvent, and for ^{13}C NMR spectra, the signal of CDCl_3 (77.16 ppm) or $\text{DMSO}-d_6$ (39.52 ppm) or CD_3OD (49.05 ppm) was used as a reference. ^{13}C NMR spectra interpretations were supported by DEPT experiments. Mass spectra were obtained on a spectrometer equipped with CI, EI, and FAB probes and on a spectrometer equipped with ESI probe. HRMS results were obtained on MALDI-TOF and ESI mass spectrometers. IR spectra were recorded on FTIR spectrometer. Optical activity of the chiral molecules was measured in a polarimeter equipped with optical rotation 1 dc cell. The progress of reactions was monitored by TLC (SiO_2) and visualized by UV light. Flash chromatography was carried out on columns packed with SiO_2 (0.04–0.063 mm). Purity of all synthesized compounds was established by HPLC and in all cases was above 96%.

tert-Butyl-2-(2-(2-aminoethoxy)ethoxy)ethylcarbamate (1). To a solution of 2,2'-(ethylenedioxy)-bis-ethylamine (2.0 g, 13.50 mmol) in dry CHCl_3 (20.0 mL), a solution of di-*tert*-butyldicarbonate (295 mg, 1.35 mmol) in CHCl_3 (20.0 mL) was added dropwise at 0 $^\circ\text{C}$ under inert atmosphere. At the end of the addition, the reaction mixture was allowed to warm up to rt and was stirred for overnight. After that time, solvents were evaporated, water (20 mL) was added, and the mixture was extracted with CH_2Cl_2 (3×20 mL). The combined organic fractions were dried over MgSO_4 and evaporated to afford **1** as light-yellow oil (328 mg, 98%). ^1H NMR (400 MHz, CDCl_3): δ 1.43 (s, 9H), 2.87 (t, $J = 5.0$ Hz, 2H), 3.30–3.33 (m, 2H), 3.50–3.55 (m, 4H), 3.61 (s, 4H). ^{13}C NMR (100 MHz, CDCl_3): δ 28.2, 40.1, 41.49, 70.0, 73.2, 78.8, 155.8. IR (film): 3056, 2987, 1265, 740 cm^{-1} . MS(CI^+): m/z 249 (MH^+). HRMS (MALDI): m/z calcd for $\text{C}_{11}\text{H}_{25}\text{N}_2\text{O}_4$, 249.1808; found, 249.1793.

tert-Butyl 2-(2-(2-(4-Hydroxybenzamido)ethoxy)ethoxy)ethylcarbamate (2). To a solution of **1** (158 mg, 0.6 mmol) in a mixture of dry CH₂Cl₂ (4.0 mL) and dry CH₃CN (4.0 mL), 4-hydroxybenzoic acid (124 mg, 0.9 mmol), HBTU (226 mg, 0.72 mmol), HOBT (81 mg, 0.72 mmol), and *N,N*-diisopropylethylamine (314 μ L, 1.8 mmol) were added at rt under inert atmosphere and the reaction mixture was stirred for 24 h. After that time, all volatiles were evaporated and the crude product was purified by column chromatography (SiO₂; CH₃OH/CH₂Cl₂, 8:92; *R*_f 0.46) to give **2** as yellow oil (200 mg, 87%). ¹H NMR (400 MHz, DMSO-*d*₆): δ 1.36 (s, 9H), 3.04 (q, *J* = 8 Hz, 2H), 3.36 (m, 4H), 3.50 (m, 6H), 3.57 (s, 1H), 6.78 (d, *J* = 8 Hz, 1H), 7.70 (d, *J* = 8 Hz, 2H), 8.22 (bs, 1H), 9.93 (s, 1H). ¹³C NMR (100 MHz, CDCl₃): δ 28.4, 38.7, 39.8, 40.3, 69.9, 70.1, 79.6, 115.5, 125.3, 129.0, 156.2, 160.2, 167.9. IR (film): 3632, 3437, 3203, 2942, 2722, 2521, 1781, 1670, 1618, 1514, 1461, 1391, 1278, 1166, 1030, 922 cm⁻¹. MS (CI⁺): *m/z* 369.0 (MH⁺). UV-vis (CH₃CN): λ_{\max} 240 nm.

(S)-tert-Butyl-2-(2-(2-(4-(2-hydroxy-2-methyl-3-(4-nitro-3-(trifluoromethyl)phenylamino)-3-oxo-propoxy)benzamido)ethoxy)ethoxy)ethylcarbamate (5). To a suspension of **3** (178 mg, 0.615 mmol) and anhydrous K₂CO₃ (170 mg, 1.230 mmol) in dry 2-butanone (5.0 mL), **2** (244 mg, 0.664 mmol) was added at rt under inert atmosphere. Then, the reaction mixture was refluxed for overnight. After that time, 2-butanone was evaporated, water (20 mL) was added, and the mixture was extracted with ethyl acetate (3 \times 20 mL). The combined organic fractions were dried over MgSO₄, and the crude product was purified by column chromatography (SiO₂; CH₃CN; *R*_f 0.3) to give **5** as yellow oil (324 mg, 80%). $[\alpha]_{\text{D}}^{20}$ -26.6° (*c* = 1.7, CH₂Cl₂). ¹H NMR (400 MHz, CDCl₃): δ 1.42 (s, 9H), 1.60 (s, 3H), 3.23 (t, *J* = 4.8 Hz, 1H), 3.51 (t, *J* = 5.2 Hz, 1H), 3.62–3.64 (m, 8H), 4.00, 4.42 (ABq, *J* = 9.2 Hz, 2H), 6.83 (d, *J* = 8.4 Hz, 2H), 7.70 (d, *J* = 7.6 Hz, 2H), 7.98 (d, *J* = 8.8 Hz, 1H), 8.06 (d, *J* = 8.8 Hz, 2H), 8.13 (bs, 1H), 9.39 (bs, 1H). ¹³C NMR (100 MHz, CDCl₃): δ 22.9, 28.3, 39.8, 40.3, 70.1, 72.8, 75.6, 79.6, 114.4, 118.3, 118.3, 122.1, 127.0, 127.0, 128.8, 141.8, 143.0, 156.1, 160.6, 167.5, 173.1. ¹⁹F NMR (376 MHz, CDCl₃): δ -60.5. IR (film): 3372, 2928, 2873, 2077, 1693, 1641, 1515, 1458, 1417, 1353, 1251, 1149, 1042, 910 cm⁻¹. HRMS (MALDI-TOF): *m/z* calcd for C₂₉H₃₇N₄O₁₀F₃Na, 681.2354; found, 681.2816. UV-vis (CH₃CN): λ_{\max} 250, 310 nm.

(S)-2-(2-(2-(4-(2-Hydroxy-2-methyl-3-(4-nitro-3-(trifluoromethyl)phenylamino)-3-oxopropoxy)benzamido)ethoxy)ethoxy)ethanaminium 2,2,2-trifluoroacetate (6). To a solution of **5** (93.6 mg, 0.412 mmol) in dry CH₃CN (2.5 mL), CF₃CO₂H (2.5 mL) was added dropwise at 0 °C under inert atmosphere. Then the reaction mixture was allowed to warm up to rt and stirred for overnight. After that time, all volatiles were evaporated and purification was performed by dissolving in minimum amount of methanol and triturated with diethyl ether to obtain the pure product **6** as light-yellow precipitate (79.3 mg, 99%). $[\alpha]_{\text{D}}^{20}$ -1.84° (*c* = 3.97, acetone). ¹H NMR (400 MHz, DMSO-*d*₆): δ 1.46 (s, 3H), 2.95 (m, 2H), 3.57 (m, 10H), 3.58, 4.28 (ABq, *J* = 8 Hz, 2H), 6.33 (bs, 1H), 6.98 (d, *J* = 8 Hz, 2H), 7.79 (d, *J* = 8 Hz, 2H), 8.12 (d, *J* = 12 Hz, 1H), 8.36 (t, *J* = 4 Hz, 1H), 8.58 (s, 1H), 10.66 (bs, 1H). ¹³C NMR (100 MHz, DMSO-*d*₆): δ 22.9, 38.5, 40.1, 66.6, 68.9, 69.3, 69.6, 73.5, 74.7, 114.0, 118.1, 118.2, 123.0, 126.7, 127.3, 128.8, 141.6, 143.1, 160.6, 165.6, 174.4. ¹⁹F NMR (376 MHz, DMSO-*d*₆): δ -59.46, -74.05. IR (film): 3434, 2928, 1684, 1535, 1422, 1352, 1251, 1193, 1142, 1038, 994, 842, 764, 725 cm⁻¹. MS (FAB⁺): *m/z* 559.2 (MH⁺). HRMS (MALDI-TOF): *m/z* calcd for C₂₄H₃₀N₄O₈F₃, 559.2010; found, 559.1997.

(S)-N-(2-(2-(2-(2-Chloroacetamido)ethoxy)ethoxy)ethyl)-4-(2-hydroxy-2-methyl-3-(4-nitro-3-(trifluoromethyl)phenylamino)-3-oxopropoxy)benzamide (7). To a solution of **6** (152 mg, 0.272 mmol) in dry CH₃CN (5.0 mL), chloroacetic anhydride (46 mg, 0.272 mmol) was added at rt under inert atmosphere. Then, the reaction mixture was heated to 35 °C for overnight. After solvent evaporation, the crude product was purified by column

chromatography (SiO₂; CH₃CN; *R*_f 0.3) to give **7** as light-yellow oil (134 mg, 95%). $[\alpha]_{\text{D}}^{20}$ +2.86 (*c* 0.05, CH₃CN). ¹H NMR (500 MHz, DMSO-*d*₆): δ 1.46 (s, 3H), 3.24 (q, *J* = 5 Hz, 2H), 3.38 (q, *J* = 5 Hz, 2H), 3.43 (t, *J* = 5 Hz, 2H), 3.52 (m, 7H), 4.05 (s, 2H), 4.06, 4.29 (ABq, *J* = 10 Hz, 2H), 6.32 (bs, 1H), 6.98 (d, *J* = 10 Hz, 2H), 7.80 (d, *J* = 10 Hz, 2H), 8.20 (d, *J* = 10 Hz, 1H), 8.25 (bs, 1H), 8.36 (m, 2H), 8.58 (d, *J* = 5 Hz, 1H), 10.66 (s, 1H). ¹³C NMR (125 MHz, DMSO-*d*₆): δ 22.94, 38.16, 38.93, 39.00, 42.48, 68.64, 68.90, 69.47, 73.52, 74.70, 113.98, 118.19, 118.23, 123.00, 126.77, 127.29, 128.87, 141.59, 143.17, 160.59, 165.58, 165.89, 174.40. ¹⁹F NMR (376 MHz, CDCl₃): δ -60.48. IR (film): 3302, 2875, 1664, 1537, 1419, 1347, 1250, 1145, 1040, 911, 844, 710 cm⁻¹. HRMS (MALDI-TOF): *m/z* calcd for C₂₆H₃₀ClF₃N₄O₉Na, 657.1551; found, 657.1596.

(S)-tert-Butyl-2,2',2''-(10-(1-(4-(2-hydroxy-2-methyl-3-(4-nitro-3-(trifluoromethyl)phenylamino)-3-oxopropoxy)phenyl)-1,12-dioxo-5,8-dioxo-2,11-diazatridecan-13-yl)-1,4,7,10-tetraazacyclododecane-1,4,7-triyl)triacetate (8). Procedure A. To a mixture of **20** (153 mg, 0.289 mmol) and KHCO₃ (40 mg, 0.289 mmol) in dry DMF (1.0 mL), a solution of **7** (183 mg, 0.289 mmol) in dry DMF (1.0 mL) was added at rt under inert atmosphere. Then, the reaction mixture was heated to 90 °C for overnight. After that time, the solvent was evaporated and the crude product was purified by column chromatography (SiO₂; MeOH:CH₂Cl₂, 1:9; *R*_f 0.3) to give **8** as light-yellow oil (225 mg, 70%). $[\alpha]_{\text{D}}^{24}$ +13.08° (*c* = 8.9, CHCl₃). ¹H NMR (500 MHz, CDCl₃): δ 1.43 (ds, 34H), 3.33–3.68 (m, 37H), 4.09 (d, *J* = 10 Hz, 1H), 4.57 (d, *J* = 10 Hz, 1H), 6.97 (d, *J* = 10 Hz, 2H), 7.42 (s, 1H), 7.64 (s, 1H), 7.78 (d, *J* = 5 Hz, 2H), 7.89 (d, *J* = 10 Hz, 1H), 8.21 (d, *J* = 10 Hz, 1H), 8.53 (s, 1H). ¹³C NMR (125 MHz, CDCl₃): δ 22.9, 27.9, 28.0, 29.7, 31.9, 38.9, 39.7, 55.5, 55.7, 56.0, 69.5, 70.0, 70.2, 70.3, 73.4, 81.8, 81.9, 114.8, 118.7, 118.8, 122.8, 126.6, 127.1, 128.9, 142.6, 143.0, 161.2, 167.4, 171.8, 172.4, 174.5. ¹⁹F NMR (188 MHz, MeOD): δ -63.53. IR (film): 3421, 2924, 2386, 2298, 1728, 1610, 1535, 1462, 1370, 1313, 1233, 1157, 1039, 848, 762 cm⁻¹. HRMS (MALDI-TOF): *m/z* calcd for C₅₂H₈₀N₈O₁₅F₃, 1113.5690; found, 1113.5647.

Procedure B. To a mixture of **3** (100 mg, 0.345 mmol) and K₂CO₃ (48 mg, 0.690 mmol) in dry 2-butanone (5 mL), a solution of **12** (284 mg, 0.345 mmol) in dry 2-butanone (5 mL) was added at rt under inert atmosphere. Then the reaction mixture was heated to 80 °C for overnight. After that time, 2-butanone was evaporated, water (15 mL) was added, and the mixture was extracted with CH₂Cl₂ (3 \times 15 mL). The combined organic fractions were dried over MgSO₄, and the crude product was purified by column chromatography to give **8** as yellow oil (345 mg, 90%).

(S)-2,2',2''-(10-(1-(4-(2-Hydroxy-2-methyl-3-(4-nitro-3-(trifluoromethyl)phenylamino)-3-oxopropoxy)phenyl)-1,12-dioxo-5,8-dioxo-2,11-diazatridecan-13-yl)-1,4,7,10-tetraazacyclododecane-1,4,7-triyl)triacetic Acid (9). To a solution of **8** (300 mg, 0.270 mmol) in dry CH₃CN (10.0 mL), CF₃CO₂H (10.0 mL) was added dropwise at 0 °C under inert atmosphere. Then, the reaction mixture was allowed to warm up to rt and stirred for overnight. After that time, all volatiles were evaporated and purification was performed by dissolving in minimum amount of methanol and triturated with diethyl ether to obtain the pure product **9** as light-yellow precipitate solid (229 mg, 90%); mp 144.3–145.5 °C. $[\alpha]_{\text{D}}^{20}$ -8.3° (*c* 4.3, MeOH). ¹H NMR (500 MHz, CD₃OD): δ 1.56 (s, 3H), 3.31–3.64 (m, 39H), 4.10, 4.39 (ABq, *J* = 10 Hz, 2H), 7.01 (d, *J* = 10 Hz, 2H), 7.78 (d, *J* = 10 Hz, 2H), 8.05 (d, *J* = 10 Hz, 1H), 8.18 (dd, *J* = 5 Hz, 1H), 8.37 (s, 1H). ¹³C NMR (125 MHz, CD₃OD): δ 23.3, 40.3, 40.8, 56.5, 57.0, 57.1, 70.6, 71.3, 71.4, 75.0, 76.5, 115.6, 119.8, 119.8, 122.5, 124.4, 128.1, 128.3, 130.3, 1440, 144.3, 162.9, 169.8, 175.0, 176.1, 179.4, 179.6. ¹⁹F NMR (188 MHz, CD₃OD): δ -78.90, -63.51. IR (KBr): 3732, 2752, 2559, 2469, 2419, 2387, 2335, 2295, 2276, 2078, 1640, 1463, 1352, 1317, 1250, 1175, 1138, 1097, 1035, 974, 914, 833, 809, 768, 705, 688, 644, 612 cm⁻¹. HRMS (MALDI-TOF): *m/z* calcd for C₄₀H₅₆F₃N₈O₁₅, 945.3839; found, 945.3877.

N-(2-(2-(2-Aminoethoxy)ethoxy)ethyl)-4-hydroxybenzamide (10). To a solution of **2** (200 mg, 0.543 mmol) in dry CH₃CN (5.0 mL), trifluoroacetic acid (5.0 mL) was added dropwise at 0 °C under inert atmosphere. Then, the reaction mixture was allowed to warm up to rt and stirred for overnight. After that time, all volatiles were evaporated and purification was performed by dissolving in minimum amount of methanol and triturated with diethyl ether to obtain the pure product **10** as light-yellow precipitate (146 mg, 99%). ¹H NMR (500 MHz, CD₃OD): δ 3.07 (t, *J* = 5 Hz, 2H), 3.56 (t, *J* = 5 Hz, 2H), 3.67 (m, 8H), 6.83 (d, *J* = 10 Hz, 2H), 7.71 (d, *J* = 10 Hz, 2H), 8.26 (s, NH). ¹³C NMR (125 MHz, CD₃OD): δ 40.63, 40.68, 67.90, 70.78, 71.37, 71.42, 116.14, 126.35, 130.27, 162.16, 170.24. IR (film): 612, 687, 772, 849, 1027, 1134, 1611, 3310 cm⁻¹. MS(CI⁺): *m/z* 269.3 (MH⁺). UV-vis (CH₃OH): λ_{max} 245 nm.

N-(2-(2-(2-Chloroacetamido)ethoxy)ethoxy)ethyl)-4-hydroxybenzamide (11). To a solution of **10** (200 mg, 0.746 mmol) and NEt₃ (206 μL, 1.49 mmol) in dry CH₃CN (3.0 mL), a solution of chloro-acetic anhydride (127 mg, 0.746 mmol) in dry CH₃CN (5 mL) was added dropwise at 0 °C under inert atmosphere. Then, the reaction mixture was allowed to warm up to rt and stirred for overnight. After that time, all volatiles were evaporated and the crude product was purified by column chromatography (SiO₂; MeOH:CH₂Cl₂, 1:9; *R_f* 0.8) to give **11** as white oil (205 mg, 80%). ¹H NMR (400 MHz, CD₃OD): δ 3.39 (t, *J* = 5.6 Hz, 4H), 3.55 (m, 4H), 3.63 (m, 4H), 4.03 (s, 2H), 6.82 (d, *J* = 8.8 Hz, 2H), 7.71 (d, *J* = 8.8 Hz, 2H). ¹³C NMR (125 MHz, CD₃OD): δ 40.7, 40.8, 43.2, 70.3, 70.8, 71.4, 116.1, 126.4, 130.3, 162.1, 169.4, 170.2. IR (film): 3323, 2873, 1643, 1607, 1278, 1098, 850, 770 cm⁻¹. HRMS (MALDI-TOF): *m/z* calcd for C₁₅H₂₁N₂O₅NaCl, 367.1037; found, 367.0998. UV-vis (CH₃OH): λ_{max} 205, 255 nm.

tert-Butyl-2,2',2''-(10-(1-(4-hydroxyphenyl)-1,12-dioxo-5,8-dioxo-2,11-diazatridecan-13-yl)-1,4,7,10-tetraazacyclododecane-1,4,7-triyl)triacetate (12). To a mixture of **20** (153 mg, 0.289 mmol) and KHCO₃ (40 mg, 0.289 mmol) in dry DMF (0.5 mL), a solution of **11** (99 mg, 0.289 mmol) in dry DMF (1 mL) was added at rt under inert atmosphere. Then, the reaction mixture was heated to 90 °C for overnight. After that time, the solvent was evaporated and the crude product was purified by column chromatography (SiO₂; MeOH:CH₂Cl₂, 1:9; *R_f* 0.3) to give **12** as light-yellow oil (190 mg, 80% yield). ¹H NMR (500 MHz, CDCl₃): δ 1.44 (s, 27H), 2.79–3.67 (m, 38H), 6.97 (d, *J* = 10 Hz, 1H), 7.03 (d, *J* = 10 Hz, 1H), 7.50 (s, NH), 7.71 (t, *J* = 10 Hz, 2H), 8.42 (s, NH). ¹³C NMR (125 MHz, CDCl₃): δ 27.99, 39.02, 39.60, 55.48, 55.64, 56.42, 57.88, 69.35, 69.85, 69.90, 70.11, 70.36, 81.19, 116.45, 122.86, 128.96, 129.03, 162.47, 168.03, 171.80, 171.84, 172.33. IR (film): 3292, 2976, 2824, 1729, 1677, 1550, 1506, 1458, 1375, 1312, 1232, 1165, 852, 757 cm⁻¹. HRMS (MALDI-TOF): *m/z* calcd for C₄₁H₇₀N₆O₁₁-Na, 845.4994; found, 845.4960. UV-vis (CH₃OH): λ_{max} 205, 255 nm.

2,2',2''-(10-(1-(4-Hydroxyphenyl)-1,12-dioxo-5,8-dioxo-2,11-diazatridecan-13-yl)-1,4,7,10-tetra-azacyclododecane-1,4,7-triyl)triacetic acid (13). To a solution of **12** (190 mg, 0.231 mmol) in dry CH₃CN (5.0 mL), CF₃CO₂H (5.0 mL) was added dropwise at 0 °C under inert atmosphere. Then, the reaction mixture was allowed to warm up to rt and stirred for overnight. After that time, all volatiles were evaporated and purification was performed by dissolving in minimum amount of methanol and triturated with diethyl ether to obtain the pure product **13** as light-yellow precipitate (136 mg, 97%). ¹H NMR (500 MHz, CD₃OD): δ 3.25 (m, 17H), 3.49 (t, *J* = 5 Hz, 6H), 3.59 (t, *J* = 5 Hz, 9H), 3.73 (bs, 6H), 6.78 (d, *J* = 5 Hz, 2H), 7.65 (d, *J* = 5 Hz, 2H), 8.64 (d, *J* = 5 Hz, 2H). ¹³C NMR (125 MHz, CD₃OD): δ 40.3, 40.8, 51.2, 51.2, 55.4, 55.4, 56.0, 70.4, 70.7, 71.2, 71.3, 116.2, 117.1, 119.4, 126.4, 127.0, 130.4, 142.9, 146.9, 162.1, 162.9, 163.1, 170.2. IR (film): 3441, 2927, 2873, 2366, 1684, 1509, 1407, 1316, 1205, 1135, 1088, 912, 839, 803, 771, 723, 689, 611, 518, 469 cm⁻¹. HRMS (MALDI-TOF): *m/z* calcd for

C₂₉H₄₇N₆O₁₁, 655.3303; found, 655.3190. UV-vis (CH₃OH): λ_{max} 210, 255 nm.

Compound 14. Compound **13** (20 mg, 0.031 mmol) was dissolved in water (5 mL), and the pH of the resulted solution was adjusted to 5.0 by the addition of aqueous KOH (0.1 M). Gadolinium acetate hydrate (13 mg, 0.037 mmol) was added, and the solution was stirred at 90 °C for overnight. Then, the reaction mixture was cooled to rt, its pH was adjusted to 10.0, and the excess of Gd(OH)₃ was removed by filtration. After water lyophilization, the crude product was purified by column chromatography (RP₁₈ silica gel; H₂O) to give **14** as yellow oil (23 mg, 91%). IR (KBr): 3448, 1692, 1562, 1413, 1204, 665 cm⁻¹. HRMS (MALDI-TOF): *m/z* calcd for C₂₉H₄₄N₆O₁₁Gd, 810.2304; found, 810.2364. UV-vis (CH₃OH): λ_{max} 200, 255 nm.

Compound 15. Compound **9** (50 mg, 0.053 mmol) was dissolved in water (5 mL), and the pH of the resulted solution was adjusted to 5.0 by the addition of aqueous KOH (0.1 M). Gadolinium acetate hydrate (23 mg, 0.064 mmol) was added and the solution was stirred at 90 °C for overnight. Then, the reaction mixture was cooled to rt, its pH was adjusted to 10.0, and the excess of Gd(OH)₃ was removed by filtration. After water lyophilization, the crude product was purified by column chromatography (RP₁₈ silica gel; H₂O) to give **15** as yellow oil (29 mg, 50%). [α]_D²⁶ -10.9% (*c* 3.0, MeOH). IR (KBr): 3424, 2361, 1641, 1563, 1414, 1021, 654 cm⁻¹. HRMS (MALDI-TOF): *m/z* calcd for C₄₀H₅₃F₃N₈O₁₅Gd, 1100.2823; found, 1100.2833. UV-vis (CH₃OH): λ_{max} 240, 310 nm.

Binding Experiments. Quantitative Immunoprecipitation AR Binding Assay. Purified recombinant human AR (10 μM) (H00000367-Q01, Abnova Corp.) was incubated for 30 min at room temperature with 10, 25, 50, 100, 250, and 500 μM of compound **22**, complex **14**, or with complex **15** in buffer (0.1% bovine serum albumin, 20 mM Tris, pH 7.4, 4 mM MgCl₂, 2 mM CaCl₂, 10 mM KCl). Then, the resulted samples were incubated with an anti-AR monoclonal antibody (5 μg/mL) (H00000367-M01, Abnova Corp.) for 2 h at 4 °C. This was followed by incubation with Protein G-Sepharose resin (GE Healthcare) for 1 h at 4 °C, and the resulting mixtures were centrifuged at 3000 rpm for 30 s. After centrifugation, the upper layer was collected and subjected to a high pressure liquid chromatography (HPLC) analysis, using UV-vis diode-array detector-equipped HPLC (Agilent 1100) and reversed phase analytical column (Econosphere C18, 5 μm, 4.6 mm × 250 mm) for detection of unbound **22**, complex **14**, or compound **15** in samples (elution conditions: mobile phase isocratic CH₃CN:H₂O, 50%:50%; 1 mL/min). Chromatograms were monitored at λ = 220, 245, and 300 nm, and integration values of area under the curve (AUC) of chromatographic peaks (assigned to antiandrogens) were used for calculation of data presented in the Figure 2.

Animals Preparation and Imaging. Orthotopic Prostate Tumors Implantation. C57/bl6 mice were anesthetized with ketamine (150 mg/kg) and xylazine (12 mg/kg). A lower-midline incision was made, and TRAMP C2 cells (1.5 × 10⁶ cells/100 μL) in PBS were implanted into the anterior, dorsolateral, and ventral prostate lobes using a 30 gauge needle. The prostate was returned to the abdominal cavity, and the abdominal wall was sutured. Mice were imaged by MRI at 4 weeks after the intraprostatic implantation of tumor cells.

Magnetic Resonance Imaging. MRI experiments were performed on 7 T BioSpec Magnet 70/30 USR system equipped with gradient coil system, capable of producing pulse gradient of up to 40 gauss/cm in each of the three directions. Mice were anesthetized with 2% inhalation anesthesia (isoflurane) delivered with oxygen, using a nonbreathing anesthetic delivery system. Anesthetized mice were placed on a heating pad to maintain normal body temperature and to minimize temperature-induced changes in blood flow. A 27 gauge needle was inserted into the tail vein for intravenous injection of contrast media Gadolinium complex **15** (6.25 mM). The MRI protocol included transverse T₁-weighted MR images. The T₁-weighted

images were acquired for tumor using the MSME sequence with a repetition delay (TR) of 700 ms, an echo delay (TE) of 11.3 ms, matrix dimension of 128 × 128 and one average, corresponding to an image acquisition time of 34 s. Twenty-four continuous slices with slice thickness of 1 mm were acquired with a field of view (FOV) of 4.5 cm × 4.5 cm.

Acknowledgment. We thank the Israel Science Foundation and the Raymond and Beverly Sackler Institute of Biophysics at Tel Aviv University for purchasing the MRI scanner and to the Strauss Institute of Computational Imaging at Tel Aviv University for data processing. We thank the Tel Aviv University for their financial support and to the Maiman Institute for Proteome Research of Tel-Aviv University for their contribution in performing mass spectrometry analyses.

Supporting Information Available: Experimental details for synthesis of compounds **1**, **2**, **3**, and 2,5,8,11-tetraoxatridecan-13-yl-4-methylbenzenesulfonate, characterization data, ¹H NMR, ¹³C NMR, MS, FT-IR, and UV-vis spectra and HPLC data. This material is available free of charge via the Internet at <http://pubs.acs.org>.

References

- Jemal, A.; Siegel, R.; Ward, E.; Murray, T.; Xu, J. Q.; Thun, M. J. Cancer statistics. *Cancer J. Clinicians* **2007**, *57*, 43–66.
- Berrepoets, C. A.; Umar, A.; Brinkmann, A. O. Endocrine. Anti-androgens: selective androgen receptor modulators. *Mol. Cell* **2002**, *198*, 97–103.
- Chandler, J. D.; Williams, E. D.; Slavin, J. L.; Best, J. D.; Rogers, S. Expression and localization of GLUT1 and GLUT12 in prostate carcinoma. *Cancer* **2003**, *97*, 2035–2042.
- Seltzer, M. A.; Barbaric, Z.; Beldegrun, A. Comparison of helical computerized tomography, positron emission tomography and monoclonal antibody scans for evaluation of lymph node metastases in patients with prostate specific antigen relapse after treatment for localized prostate cancer. *J. Urology* **1999**, *162*, 1322–1328.
- Shreve, P. D.; Grossma, H. B.; Gross, M. D.; Wahl, R. L. Metastatic prostate cancer: initial findings of PET with 2-deoxy-2-[F-18]fluoro-D-glucose. *Radiology* **1996**, *199*, 751–756.
- Sanz, G.; Robles, J. E.; Gimenez, M. Positron emission tomography with 18-fluorine-labelled deoxyglucose: utility in localized and advanced prostate cancer. *BJU Int.* **1999**, *84*, 1028–1031.
- Kalkner, K. M.; Ginman, C.; Nilsson, S.; Bergstrom, M.; Antoni, G.; Ahlstrom, H.; Langstrom, B.; Westlin, J. E. Positron emission tomography (PET) with 11C-5-hydroxytryptophan (5-HTP) in patients with metastatic hormone-refractory prostatic adenocarcinoma. *Nucl. Med. Biol.* **1997**, *24*, 319–325.
- He, Y.; Yin, D. G.; Perera, M. A.; Kirkovsky, L.; Stourman, N.; Li, W. Novel nonsteroidal ligands with high binding affinity and potent functional activity for the androgen receptor. *Eur. J. Med. Chem.* **2002**, *37*, 619–634.
- Dalton, J. T.; Mukherjee, A.; Zhu, Z.; Kirkovsky, L.; Miller, D. D. Discovery of nonsteroidal androgens. *Biochem. Biophys. Res. Commun.* **1998**, *244*, 1–4.
- Huggins, C. Endocrine-induced regression of cancers. *Cancer Res.* **1967**, *27*, 1925–1930.
- Hallows, R.; Cox, S.; Hayward, S.; Deshpande, N.; Towler, J. Effects of flutamide and hydroxyl-flutamide on the growth of human benign prostatic hyperplasia cells in primary culture: a preliminary report. *Anticancer Res.* **1991**, *11*, 1799–1805.
- Tucker, H.; Crook, J. W.; Chesterson, G. Nonsteroidal antiandrogens. Synthesis and structure–activity relationship of 3-substituted derivatives of 2-hydroxypropionanilids. *J. Med. Chem.* **1988**, *31*, 954–959.
- James, K. D.; Ekwuribe, N. N. A two-step synthesis of the anti-cancer drug (R,S)-bicalutamide. *Synthesis* **2002**, *7*, 850–852.
- Marhefka, C. A.; Moore, B. M.; Bishop, T. C.; Kirkovsky, L.; Mukherjee, A.; Dalton, J. T.; Miller, D. D. Homology modeling using multiple molecular dynamics simulations and docking studies of the human androgen receptor ligand binding domain bound to testosterone and nonsteroidal ligands. *J. Med. Chem.* **2001**, *44*, 1729–1740.
- Söderholm, A. A.; Lehtovuori, P. T.; Nyrönen, T. H. Three-dimensional structure–activity relationships of nonsteroidal ligands in complex with androgen receptor ligand-binding domain. *J. Med. Chem.* **2005**, *48*, 917–925.
- Yin, D.; He, Y.; Perera, M. A.; Hong, S. S.; Marhefka, C.; Stourman, N.; Kirkovsky, L.; Miller, D. D.; Dalton, J. T. Key Structural Features of Nonsteroidal Ligands for Binding and Activation of the Androgen Receptor. *Mol. Pharmaceutics* **2003**, *63*, 211–223.
- Marhefka, C. A.; Gao, W.; Chung, K.; Kim, J.; He, Y.; Yin, D.; Bohl, C.; Dalton, J. T.; Miller, D. D. Design, synthesis, and biological characterization of metabolically stable selective androgen receptor modulators. *J. Med. Chem.* **2004**, *47*, 993–998.
- Kattan, M.; Stapleton, A.; Wheeler, T.; Scardino, P. Evaluation of a nomogram used to predict the pathologic stage of clinically localized prostate carcinoma. *Cancer* **1997**, *79*, 528–537.
- Kattan, M. W.; Eastham, J. A.; Stapleton, A. M.; Wheeler, T. M.; Scardino, P. T. A preoperative nomogram for disease recurrence following radical prostatectomy for prostate cancer. *J. Natl. Cancer Inst.* **1998**, *90*, 766–771.
- Kattan, M. W.; Zelefsky, M. J.; Kupelian, P. A.; Scardino, P. T.; Fuks, Z.; Leibel, S. A. Pretreatment nomogram for predicting the outcome of three-dimensional conformal radiotherapy in prostate cancer. *J. Clin. Oncol.* **2000**, *18*, 3352–3359.
- Stephenson, A. J.; Shariat, S. F.; Zelefsky, M. J. Salvage radiotherapy for recurrent prostate cancer after radical prostatectomy. *JAMA, J. Am. Med. Assoc.* **2004**, *291*, 1325–1332.
- Deb, N.; Goris, M.; Trisler, K. Treatment of hormone-refractory prostate cancer with 90Y-CYT-356 monoclonal antibody. *Clin. Cancer Res.* **1996**, *2*, 1289–1297.
- Larson, S. M.; Morris, M.; Gunther, I.; Beattie, B.; Humm, J. L.; Akhurst, T. A.; Finn, R. D.; Erdi, Y.; Pentlow, K.; Dyke, J.; Squire, O.; Bornmann, W.; McCarthy, T.; Welch, M.; Scher, H. Tumor localization of 16beta-18F-fluoro-5alpha-dihydrotestosterone versus 18F-FDG in patients with progressive, metastatic prostate cancer. *J. Nucl. Med.* **2004**, *45*, 366–373.
- Zanzonico, P. B.; Finn, R.; Pentlow, K. S.; Erdi, Y.; Beattie, B.; Akhurst, T.; Squire, O.; Morris, M.; Scher, H.; McCarthy, T.; Welch, M.; Larson, S. M.; Humm, J. L. PET based radiation dosimetry in man of 18F-Fluorodihydrotestosterone, a new radiotracer for imaging prostate cancer. *J. Nucl. Med.* **2004**, *45*, 1966–1971.
- Jacobson, O.; Bechor, Y.; Icar, A.; Novak, N.; Birman, A.; Marom, H.; Fadeeva, L.; Golan, E.; Leibovitch, I.; Gutman, M.; Even-Sapir, E.; Chisin, R.; Gozin, M.; Mishani, E. Prostate cancer PET bioprobes: Synthesis of [18F]-radiolabeled hydroxyflutamide derivatives. *Bioorg. Med. Chem.* **2005**, *13*, 6195–6205.
- Jacobson, O.; Laky, D.; Carlson, K. E.; Elgavish, S.; Gozin, M.; Even-Sapir, E.; Leibovitch, I.; Gutman, M.; Chisin, R.; Katzenellenbogen, J. A.; Mishani, E. Chiral dimethylamine flutamide derivatives—modeling, synthesis, androgen receptor affinities and carbon-11 labeling. *Nucl. Med. Biol.* **2006**, *33*, 695–704.
- Parent, E. E.; Jenks, C.; Sharp, T.; Welch, M. J.; Katzenellenbogen, J. A. Synthesis and biological evaluation of a nonsteroidal bromine-76-labeled androgen receptor ligand 3-[76Br]bromo-hydroxyflutamide. *Nucl. Med. Biol.* **2006**, *33*, 705–713.
- Parent, E. E.; Dence, C. S.; Jenks, C.; Sharp, T. L.; Welch, M. J.; Katzenellenbogen, J. A. Synthesis and Biological Evaluation of [18F]Bicalutamide, 4-[76Br]Bromobicalutamide, and 4-[76Br]-Bromo-thiobicalutamide as Nonsteroidal Androgens for Prostate Cancer Imaging. *J. Med. Chem.* **2007**, *50*, 1028–1040.
- He, H.; Morely, J. E.; Silva-Lopez, E.; Bottenus, B.; Montajano, M.; Fugate, G. A.; Twamley, B.; Benny, P. D. Synthesis and Characterization of Nonsteroidal-Linked M(CO)³⁺ (M = ^{99m}Tc, Re) Compounds Based on the Androgen Receptor Targeting Molecule Flutamide. *Bioconjugate Chem.* **2009**, *20* (1), 78–86.
- Dehdashti, F.; Picus, J.; Michalski, J. M.; Dence, C. S.; Siegel, B. A.; Katzenellenbogen, J. A.; Welch, M. J. Positron tomographic assessment of androgen receptors in prostatic carcinoma. *Eur. J. Nucl. Med. Mol. Imaging* **2005**, *32*, 344–350.
- Sillerud, L. O. Magnetic resonance imaging of prostate cancer. Pat. Appl. US 2006140871, 2006, 20 pp.
- Frangioni, J. V. Modified PSMA ligands for diagnosis and treatment of prostate cancer. PCT Int. Appl. WO 2002098885, 2002, 72 pp.
- John, C. S.; Vilner, B. J.; Geyer, B. C.; Moody, T.; Bowen, W. D. Targeting sigma receptor-binding benzamides as in vivo diagnostic and therapeutic agents for human prostate tumors. *Cancer Res.* **1999**, *59*, 4578–4583.
- Glen, A. T.; Hughes, L. R.; Morris, J. J.; Taylor, P. J. Nonsteroidal Antiandrogens. Design of novel compounds based on an infrared study of the dominant conformation and hydrogen bonding properties of a series of anilide antiandrogens. *J. Med. Chem.* **1991**, *34*, 447–455.
- Patil, R.; Li, W.; Ross, C. R., II; Kraka, E.; Cremer, D.; Mohler, M. L.; Dalton, J. T.; Miller, D. D. Cesium fluoride and

- tetra-*n*-butylammonium fluoride mediated 1,4-NO shift of disubstituted phenyl ring of a bicalutamide derivative. *Tetrahedron Lett.* **2006**, *47*, 3941–3944.
- (36) Bohl, C. E.; Wu, Z.; Miller, D. D.; Bell, C. E.; Dalton, J. T. Crystal Structure of the T877A Human Androgen Receptor Ligand-Binding Domain Complexed to Cyproterone Acetate Provides Insight for Ligand-Induced Conformational Changes and Structure-Based Drug Design. *J. Biol. Chem.* **2007**, *282* (18), 13648–13655.
- (37) Yang, J.; Bohl, C. E.; Nair, V. A.; Mustafa, S. M.; Hong, S. S.; Miller, D. D.; Dalton, J. T. Preclinical pharmacology of a non-steroidal ligand for androgen receptor-mediated imaging of prostate cancer. *J. Pharmacol. Exp. Ther.* **2006**, *317* (1), 402–408.
- (38) Bohl, C. E.; Miller, D. D.; Chen, J.; Bell, C. E.; Dalton, J. T. Structural Basis for Accommodation of Nonsteroidal Ligands in the Androgen Receptor. *J. Biol. Chem.* **2005**, *280* (45), 37747–37754.
- (39) Nair, V. A.; Mustafa, S. M.; Mohler, M. L.; Yang, J.; Kirkovsky, L. I.; Dalton, J. T.; Miller, D. D. Synthesis of irreversibly binding bicalutamide analogs for imaging studies. *Tetrahedron Lett.* **2005**, *46*, 4821–4823.
- (40) Bohl, C. E.; Gao, W.; Miller, D. D.; Bell, C. E.; Dalton, J. T. Structural basis for antagonism and resistance of bicalutamide in prostate cancer. *Proc. Natl. Acad. Sci. U.S.A.* **2005**, *102* (17), 6201–6206.
- (41) Krasnow, N. Effects of lanthanum and gadolinium ions on cardiac sarcoplasmic reticulum. *Biochim. Biophys. Acta* **1972**, *282*, 187–194.
- (42) Zhang, H.; Schuhmacher, J.; Waser, B.; Wild, D.; Eisenhut, M.; Reubi, J. Claude.; Maecke, H. R. DOTA-PESIN, a DOTA-conjugated bombesin derivative designed for the imaging and targeted radionuclide treatment of bombesin receptor-positive tumours. *Eur. J. Nucl. Med. Mol. Imaging* **2007**, *34*, 1198–1208.
- (43) Maecke, H. R.; Hofmann, M.; Haberkorn, U. ⁶⁸Ga-labeled peptides in tumor imaging. *J. Nucl. Med.* **2005**, *46*, 172–175.
- (44) Li, C.; Wen, X.; Wu, Q.-P.; Wallace, S.; Ellis, L. M. Diagnostic imaging compositions, their methods of synthesis, and use. PCT Int. Appl. WO 2002087498, 2002, 84 pp.
- (45) Zheng-Rong, L.; Xinghe, W.; Parker, D. L.; Goodrich, K. C.; Buswell, H. R. Poly(L-glutamic acid) Gd(III)-DOTA Conjugate with a Degradable Spacer for Magnetic Resonance Imaging. *Bioconjugate Chem.* **2003**, *14*, 715–719.
- (46) Iten, F.; Mueller, B.; Schindler, C.; Rochlitz, C.; Oertli, D.; Maecke, H. R.; Mueller-Brand, J.; Walter, M. A. Response to [90Yttrium-DOTA]-TOC treatment is associated with long-term survival benefit in metastasized medullary thyroid cancer: a phase II clinical trial. *Clin. Cancer Res.* **2007**, *13*, 6696–6702.
- (47) Konijnenberg, M.; Melis, M.; Valkema, R.; Krenning, E.; de Jong, M. Radiation dose distribution in human kidneys by octreotides in peptide receptor radionuclide therapy. *J. Nucl. Med.* **2007**, *48*, 134–142.
- (48) Krenning, E. P.; Valkema, R.; Kooij, P. P. M.; Breeman, W. A. P.; Bakker, W. H.; De Herder, W. W.; Van Eijck, C. H. J.; Kwekkeboom, D. J.; De Jong, M.; Jamar, F.; Pauwels, S. The role of radioactive somatostatin and its analogues in the control of tumor growth. *Recent Results Cancer Res.* **2000**, *153*, 1–13.
- (49) Dalton, J. T.; Miller, D. D.; He, Y.; Yin, D. Method for preparation of *N*-[4-nitro-3-(trifluoro-methyl)phenyl]-(2*S*)-3-[4-(acetyl-amino)phenoxy]-2-hydroxy-2-methylpropanamide and related compounds as selective androgen receptor modulators. Pat. Appl. US 2004014975, 2004, 29 pp.
- (50) Walters, I.; Bennion, C.; Connolly, S.; Croshaw, P. J.; Hardy, K.; Hartopp, P.; Jackson, C. G.; King, S. J.; Lawrence, L.; Mete, A.; Murray, D.; Robinson, D. H.; Stein, L.; Wells, E.; Withnall, W. J. Synthesis and evaluation of substrate-mimicking cytosolic phospholipase A2 inhibitors—reducing the lipophilicity of the arachidonyl chain isostere. *Bioorg. Med. Chem. Lett.* **2004**, *14*, 3645–3649.
- (51) Beer, P. D.; Cadman, J.; Lloris, J. M.; Martinez-Manez, R.; Soto, J.; Pardo, T.; Marcos, M. D. Anion interaction with ferrocene-functionalized cyclic and open-chain polyaza and aza-oxa cycloalkanes. *Dalton* **2000**, *11*, 1805–1812.
- (52) Ryckebusch, A.; Deprez-Poulain, R.; Maes, L.; Debreu-Fontaine, M.-A.; Mouray, E.; Grellier, P.; Sergheraert, C. Synthesis and in Vitro and in Vivo Antimalarial Activity of *N*1-(7-Chloro-4-quinolyl)-1,4-bis(3-aminopropyl)piperazine Derivatives. *J. Med. Chem.* **2003**, *46*, 542–557.
- (53) Pardin, C.; Gillet, S. M. F. G.; Keillor, J. W. Synthesis and evaluation of peptidic irreversible inhibitors of tissue transglutaminase. *Bioorg. Med. Chem.* **2006**, *14*, 8379–8385.
- (54) Li, C.; Law, G.-L.; Wong, W.-T. Luminescent Tb³⁺ complex with pendant crown ether showing dual-component recognition of H⁺ and K⁺ at multiple pH windows. *Org. Lett.* **2004**, *6*, 4841–4844.
- (55) Hurwitz, A. A.; Foster, B. A.; Allison, J. P.; Greenberg, N. M.; Kwon, E. D. The TRAMP mouse as a model for prostate cancer. In *Current Protocols in Immunology*; Wiley: New York, 2001; Chapter 20, Unit 20.5.
- (56) Cifuentes, E.; Mataraza, J. M.; Yoshida, B. A.; Menon, M.; Sacks, D. B.; Barrack, E. R.; Reddy, G. P. Physical and functional interaction of androgen receptor with calmodulin in prostate cancer cells. *Proc. Natl. Acad. Sci. U.S.A.* **2004**, *101* (2), 464–469.
- (57) Berger, R.; Febbo, P. G.; Majumder, P. K.; Zhao, J. J.; Mukherjee, S.; Signoretti, S.; Campbell, K. T.; Sellers, W. R.; Roberts, T. M.; Loda, M.; Golub, T. R.; Hahn, W. C. Androgen-induced differentiation and tumorigenicity of human prostate epithelial cells. *Cancer Res.* **2004**, *64* (24), 8867–8875.
- (58) Park, J. A.; Lee, J. J.; Jung, J. C.; Yu, D. Y.; Oh, C.; Ha, S.; Kim, T. J.; Chang, Y. Gd-DOTA conjugate of RGD as a potential tumor-targeting MRI contrast agent. *ChemBioChem* **2008**, *9* (17), 2811–2813.